

#### **PAPER • OPEN ACCESS**

A method for using Josephson voltage standards for direct characterization of high performance digitizers to establish AC voltage and current traceability to SI

To cite this article: J Ireland et al 2023 Meas. Sci. Technol. 34 015003

View the article online for updates and enhancements.

# You may also like

- Calibration of ultrastable low-noise current amplifiers without direct use of a cryogenic current comparator
   M Götz, D Drung, C Krause et al.
- Effects of differences in hardness measurement procedures on the traceability chain and calibration process Nae Hyung Tak, Hae Moo Lee and Gunwoong Bahng
- New traceability chain for spectral irradiance measurement at LNE-Cnam Mai Huong Valin, Gaël Obein, Bernard Rougie et al.



Meas. Sci. Technol. 34 (2023) 015003 (17pp)

https://doi.org/10.1088/1361-6501/ac9542

# A method for using Josephson voltage standards for direct characterization of high performance digitizers to establish AC voltage and current traceability to SI

J Ireland<sup>1,\*</sup>, P G Reuvekamp<sup>1</sup>, J M Williams<sup>1</sup>, D Peral<sup>2</sup>, J Díaz de Aguilar<sup>2</sup>, Y A Sanmamed<sup>2</sup>, M Šíra<sup>3</sup>, S Mašláň<sup>3</sup>, W Rzodkiewicz<sup>4</sup>, P Bruszewski<sup>4</sup>, G Sadkowski<sup>4</sup>, A Sosso<sup>5</sup>, V Cabral<sup>6</sup>, H Malmbekk<sup>7</sup>, A Pokatilov<sup>8</sup>, J Herick<sup>9</sup>, R Behr<sup>9</sup>, T Coşkun Öztürk<sup>10</sup>, M Arifovic<sup>10</sup> and D Ilić<sup>11</sup>

E-mail: jane.ireland@npl.co.uk

Received 31 May 2022, revised 30 August 2022 Accepted for publication 27 September 2022 Published 19 October 2022



# **Abstract**

A method for traceability to SI for ac voltage and current based on high performance digitizers is presented. In contrast to the existing thermal-based methods, the proposed method utilizes direct traceability to quantum-based waveforms via the use of Josephson voltage systems. This allows not only a simplification of the traceability chain and reduced measurement times but also offers the potential for analysis of the ac voltage and current waveform spectral content, a feature which is not possible using thermal methods. Scaling of current and voltage is achieved by the use of current shunts and resistive voltage dividers respectively. Target operating ranges are up to 1 A and 100 V with a frequency range up to 1 kHz for both. The corresponding target uncertainty for this traceability route is 1  $\mu$ V V<sup>-1</sup> and 2  $\mu$ A A<sup>-1</sup> up to frequencies of 1 kHz. The traceability chain is described and various components are characterized to validate their suitability for this task. It is demonstrated that these uncertainty targets can be met under certain conditions. The use of multi-tone calibration waveforms is investigated to further reduce

Original Content from this work may be used under the terms of the Creative Commons Attribution 4.0 licence. Any

further distribution of this work must maintain attribution to the author(s) and the title of the work, journal citation and DOI.

National Physical Laboratory, Hampton Road, Teddington, Middlesex TW11 0LW, United Kingdom

<sup>&</sup>lt;sup>2</sup> CEM, Spanish Center of Metrology, del Alfar 2, 28760 Tres Cantos, Madrid, Spain

<sup>&</sup>lt;sup>3</sup> Czech Metrological Institute, Okružní 31, 636 00 Brno, Czech Republic

<sup>&</sup>lt;sup>4</sup> GUM, Central Office of Measures, Elektoralna 2, 00-139 Warsaw, Poland

<sup>&</sup>lt;sup>5</sup> INRiM, Strada delle Cacce 91, 10135 Torino, Italy

<sup>&</sup>lt;sup>6</sup> Instituto Português da Qualidade (IPQ), Rua António Gião 2, 2829-513 Caparica, Portugal

<sup>&</sup>lt;sup>7</sup> Justervesenet, Fetveien 99, 2007 Kjeller, Norway

<sup>&</sup>lt;sup>8</sup> AS Metrosert, 12618 Tallinn, Estonia

<sup>&</sup>lt;sup>9</sup> Physikalisch-Technische Bundesanstalt (PTB), Bundesallee 100, 38116 Braunschweig, Germany

<sup>&</sup>lt;sup>10</sup> TÜBİTAK Ulusal Metroloji Enstitüsü (UME), P.K. 54, 41470 Gebze-Kocaeli, Turkey

<sup>&</sup>lt;sup>11</sup> Faculty of Electrical Engineering and Computing, Primary Electromagnetic Laboratory (FER-PEL), Unska 3, HR-10000 Zagreb, Croatia

Author to whom any correspondence should be addressed.

measurement time. An uncertainty analysis method based on simulation using real component performance data is demonstrated.

Keywords: Josephson voltage, thermal voltage converter, digitizer, voltage measurement, quantum Hall resistance

(Some figures may appear in colour only in the online journal)

## 1. Introduction

The Josephson voltage standard (JVS) and the Quantum Hall Resistance (QHR) have been used for the dc Volt and resistance at National Measurement Institutes (NMIs) for many decades, using the values adopted by the BIPM in 1990 for the von Klitzing constant  $R_{K-90}$  and the Josephson constant  $K_{\rm J-90}$ . With the redefinition of the SI in 2019 [1] all units are now defined by fixed numerical values of the defining constants. In particular, e (elementary charge) and h (Planck's constant) are used for a practical realization of the ampere based on the Josephson and quantum Hall effects [2]. Typically an uncertainty of the order of 1 nV can be achieved on a 10 V dc measurement (k=2) [3]. However, the same is not true of ac voltage where NMIs typically rely on thermal-based methods for dissemination of the scale (figure 1(a)). A thermal voltage converter (TVC) is used as an ac-dc transfer standard [4, 5] and a typical uncertainty on the amplitude of a 1 V sinusoidal ac voltage waveform of frequency 1 kHz is of the order of 2  $\mu$ V V<sup>-1</sup> to 4  $\mu$ V V<sup>-1</sup> (k = 2) [3]. The TVC is used to obtain the dc voltage that results in the same heating as an applied ac voltage. Traceability to the SI is obtained using a dc voltage transfer standard (for example a Zener reference standard) which has been calibrated against a dc JVS to provide the reference rms voltage value. This thermal method is time consuming as it requires averaging each set of measurements over a time period of the order of 1 h. In contrast to the intrinsic standards (JVS, QHR), the TVC output is subject to drift over time. Therefore to utilize TVCs in the traceability chain, historic knowledge of their stability over long periods of time is required as well as the calculable value of the ac-dc difference. The thermal method provides only the rms value of the voltage waveform and therefore cannot provide any spectral information. An alternative to the use of thermal devices in the ac voltage and current traceability chain is to transfer the scale directly to a high-performance digitizer from a JVS [6]. High-performance digitizers, ac Josephson systems and their combined use with TVCs has been subject to a large body of research, briefly described below.

JVSs are in widespread use globally both at NMIs and at top tier research and calibration laboratories (for a general review see [7] or [8]). AC Josephson systems have been developed using either programmable Josephson voltage standards (PJVSs) [9] or Josephson Arbitrary Waveform Synthesizers (JAWS) [10].

High-performance digitizers in common use in electrical metrology include the National Instruments NI5922 and the Keysight 3458A (for a thorough review see [11]). These digitizers are used in this work and have previously been the

subject of several investigations using TVCs. For example, the use of a TVC to characterize the NI5922 digitizer is described in [12–14]. Josephson systems have also been used to calibrate TVCs. For example, [6, 15] use PJVS and [16] uses JAWS to calibrate a TVC.

There has been significant interest in the use of JVSs to characterize the performance of digitizers, particularly for use in power measurements. Examples include the use of a PJVS to characterize the NI5922 digitizer [17], the 3458A [18–22] and the Fluke 8558A [23]. A Primary AC Power Standard based on a PJVS has been developed [24] and an ac power standard comparison with PJVS and JAWS has been undertaken [25]. There is ongoing research into a quantum-based power standard [26]. JAWS systems have been used to characterize both the NI5922 [27, 28] and the 3458A [29, 30] at higher frequencies.

The new method for traceability proposed in this work is shown in figure 1(b). This method builds on the work described above and uses JVSs to directly calibrate the digitizer, operating under certain conditions, using a set of precisely known voltage waveforms. This provides direct traceability to the SI. For ac current and voltage measurements, specific current shunts and voltage dividers are used and TVCs are replaced by digitizers. For inputs outside the calibrated range of the digitizer the current shunt or divider is used as a scaling device to access a wide range of possible input currents and voltages. We here describe this proposed new traceability route for current and voltage based directly on Josephson standards and present measurements on the components of the system including digitizers and scaling devices. We also describe the measurement software and algorithms used to obtain results as well as calculate uncertainties. The motivation is to reduce measurement times and reduce uncertainties in some parameter ranges. The method is more flexible allowing future spectral characterisation of instruments using Josephson based systems. There is also the ambition to construct an agreed European system for digital traceability using this method [31]. This system is based on a shared hardware, software and data analysis process across several NMIs.

This paper consists of three sections. The measurement setup required for the proposed traceability chain is described in section 2. It provides details of the requirements for each of the components of the system, including JVSs, digitizers, ac current and voltage sources, voltage dividers, current shunts and sampling and data analysis software. In section 3 the results of the validation of various system components is given. In section 4 the software used to calculate uncertainties from real system parameters is described.

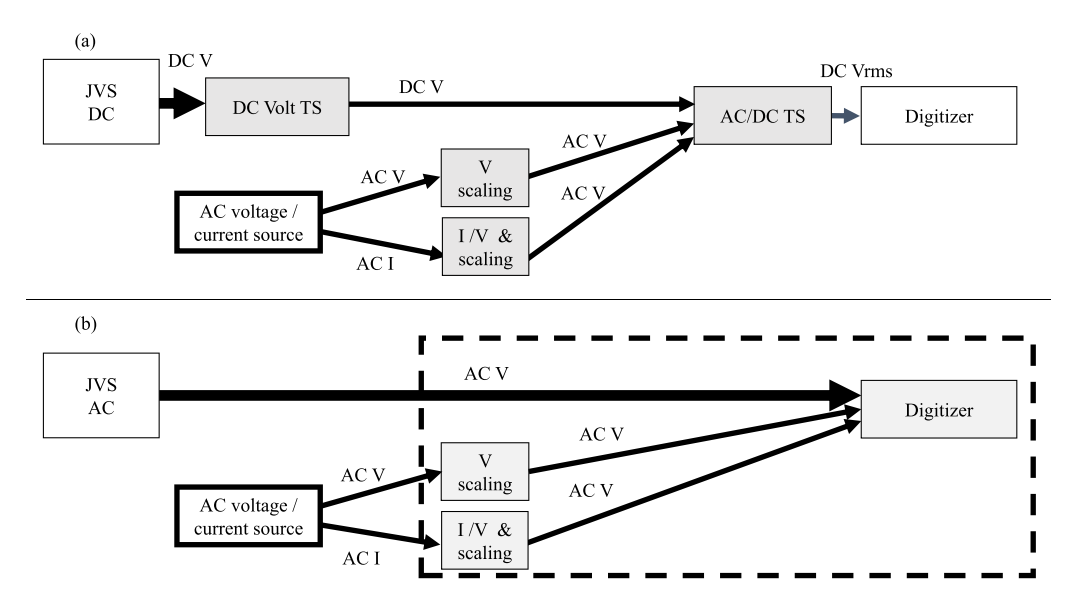


**Figure 1.** Traceability route for ac current and voltage at an NMI for (a) existing route and (b) route proposed in this work. In (a) the Josephson Voltage Standard (JVS) provides calibration of a dc voltage transfer standard (DC Volt TS) which is applied to the thermal voltage converter transfer standard (AC/DC TS) and measured by a digitizer. This is compared with the output of the ac current/voltage source under test which is applied to the AC/DC TS via voltage or current scaling devices (if required) and a current to voltage converting device (current shunt) in the case of current. In this way the output of the ac voltage/current source is traceable to the SI via thermal methods. In (b) the output of the ac current/voltage source combined with the scaling and converting device is applied directly to the digitizer. A JVS is used to characterize the dynamic performance of the digitizer providing direct traceability to the SI. Grey shading denotes items that require characterization. Thick arrows show traceability to the SI via the Josephson effect. DC V, AC V and AC I denote dc voltage and ac voltage and current waveforms respectively. Items characterized in this work are shown in the dashed box.

## 2. Measurement setup

We describe the measurement configuration required by an NMI to deliver the traceability route shown in figure 1(b)<sup>12</sup>. In this proposed new route, an industrial user requiring traceability will benefit from the reduced steps in their traceability chain as shown in figure 2(b) compared to the existing route shown in figure 2(a). The industrial user requires the NMI to calibrate their digitizer, voltage divider and current shunt. Computer software to sample data using the digitizer and analyse the results is also required. These items are described below.

#### 2.1. JVSs

The typical operating parameters of the two types of Josephson system used in this work are shown in table 1. The PJVS can be utilized at frequencies up to 1 kHz whilst the JAWS can be used up into the megahertz range.

2.1.1. Programmable JVS. The PJVS systems used in this work are described in more detail in [9, 32, 33]. PJVS systems use a Josephson Junction array which utilize a microwave source (operating at around 20 GHz or 70 GHz) in conjunction with a bias source to generate a step-wise waveform. The microwave source and bias source are both locked to a master clock. A particular feature of the system described in [9] is the

ability to use either the direct output of the PJVS (a step-wise waveform) or to use a quantum-referenced continuous waveform produced by a digital to analog converter locked to the output of the PJVS. This continuous waveform can be matched to the signal under test (a sine wave) to within the limit of the smallest voltage output of the array. Although this feature is not utilized in this work, the feature demands that the PJVS system must generate the step-wise waveform at the same rate as the continuous waveform electronics. The continuous waveform electronics operate at a fixed rate of 100 kHz therefore the sample rate must also be 100 kHz. This places restrictions on the use of this particular PJVS system to characterize digitizers as described in section 3.1.

The basic principle of JAWS can be described 2.1.2. JAWS. as follows: a current pulse, with a time dependent pulserepetition frequency  $f_p(t)$  transfers N flux quanta  $\Phi_0$  through M Josephson junctions [10]. The signal voltage V(t) in pulse-mode operation can be calculated using the Josephson equation:  $V(t) = N \cdot M \cdot \Phi_0 \cdot f_p(t)$ . According to this equation a quantized, time-dependent voltage is generated at the junction series array output leads, because only flux quanta  $\Phi_0 = h/2e$ are transferred and N and M are integer numbers. Typically, the modulator frequency corresponds to the characteristic frequency of the Josephson junctions, about 15 GHz, and provides large oversampling ratios up to frequencies of 1 MHz. On-chip filters exploit superconducting inductances to filter quantization noise at the output used for metrological purposes [34] which are typically analysed by a commercial high speed digitizer. A higher-order sigma-delta modulation

<sup>&</sup>lt;sup>12</sup> Identification of commercial equipment does not imply an endorsement by the authors or that it is the only available solution.

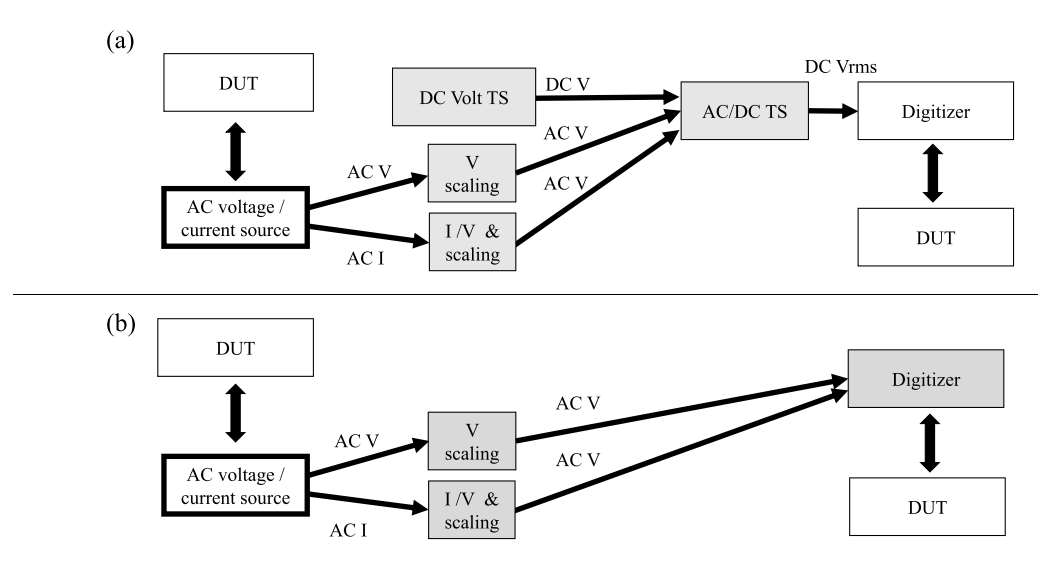


**Figure 2.** Schematic diagrams showing the traceability route at an industrial user laboratory to calibrate a device under test (DUT) for example a digitizer or ac source. The DUT is interchanged with the digitizer or ac source used to establish traceability (shown with double-headed arrows) (a) denotes the existing and (b) the proposed route. The grey items are items that have been characterized by an NMI against Josephson standards as described in this work.

**Table 1.** Operation parameters of the Josephson voltage systems used in this work; PJVS (programmable Josephson voltage standard) and JAWS (Josephson arbitrary waveform synthesizer which is based on a pulse-driven Josephson array).

	PJVS	JAWS
Frequency (Hz) Voltage (V)	dc to 1 kHz $\pm 10 \text{ V}$	dc to 1 MHz ±1 V <sub>rms</sub>

[35] is used to digitize analog waveforms into a bit pattern containing +1, 0 and -1. Commercial Pulse Pattern Generators are used to store these patterns of positive and negative current pulses that generate the desired waveform across the M Josephson junctions in the series array. As transfer of a flux-quanta ( $\Phi_0 \approx 2 \,\mu\text{V GHz}^{-1}$ ) delivers only a very small voltage at the typical operating frequency of 15 GHz, many Josephson junctions implemented in a series array are necessary to achieve practicable large output voltages. Recently a maximum voltage of 4 V rms was achieved [36]. In this work we either operate a single or eight JAWS arrays in series to achieve higher voltages, namely 100 mV or 1 V using about 9000 or 60 000 Josephson junctions, respectively [37]. The socalled ac coupling technique [38] is used to enable the JAWS arrays to produce floating ac voltages with operating margins always larger than 0.5 mA.

# 2.2. Digitizers

Key to the success of this new traceability method is the availability of high performance digitizers that exhibit long term stable measurement capability. The digitizers considered in this project are shown in table 2 along with some typical operating parameters. Both integrating and delta sigma architecture digitizers are considered. A principle of this work is that the digitizer is characterized under a particular set of conditions

**Table 2.** Types of digitizer characterized in this work including selected typical operation parameters.

Digitizer	Type	Settings used
National instruments NI5922	Delta Sigma	2 V range, 1 MΩ input impedance, 48 tap FIR filter.
Keysight 3458A	Integrating	1 V range, 10 GΩ input impedance, DCV mode.
Fluke 8588A	Integrating, proprietary	$0.1~V$ and $10~V$ range, $10~M\Omega$ input impedance, sampling mode.

and then used with the same operating parameters for all measurements while the scaling is performed by a voltage divider or current shunt as appropriate, as described below.

# 2.3. AC voltage and current source

An arbitrary reference source of ac voltage and current is required at the industrial user lab as shown in figure 2(b). This source should be highly stable (for example see [39, 40]). However, in our proposed scheme the sources in the traceability chain can be calibrated and monitored against the quantum-traceable digitizer, significantly relaxing the accuracy and stability requirements on the reference sources. To calibrate a digitizer, the user will set the source to a fixed output and transfer the traceability from the calibrated digitizer to the digitizer under test by applying the same signal to both instruments simultaneously. Range scaling can be included as described in sections 2.4 and 2.5. Conversely, if the device requiring calibration by the user is a source, it can be directly applied to the digitizer, or via voltage divider or current shunt if required, to obtain traceability.

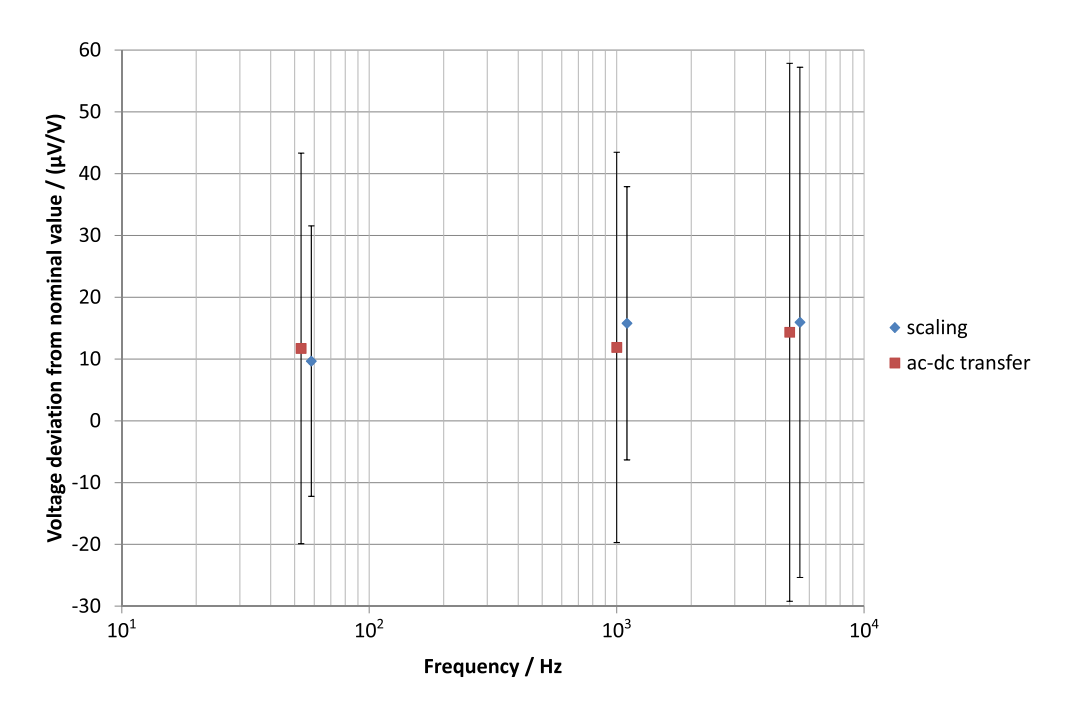


**Figure 3.** Deviation in the voltage level obtained by the scaling up procedure against the same voltage level of 220 V calibrated directly by the ac-dc transfer standard.

## 2.4. Voltage dividers

To extend the operating range of the quantum standard over the much wider interval of values required for calibration services, suitable methods for scaling are needed (figure 1(b)). A simple approach would be to use the well known analogue techniques, yet digital solutions are interesting for improving performances closer to quantum accuracy. Very successful results were obtained in dc measurements using digital multimeters based on integrating digitizers. They show extremely linear behaviour, with intrinsic accuracy better than  $0.1 \mu V V^{-1}$  and even better stability over time [41]. It is then possible to characterize the residual non-linearity of such converters using a JVS, to verify the specifications and apply further correction. A digitizer characterized against a JVS can be effectively used in place of resistive dividers in dc, but this technique cannot be transferred 'as is' to ac. Performances of analog to digital converters (ADCs) degrade as frequency increases, according to the rule: 'more speed means less resolution' that holds true for all conversion technologies, including those used in metrological labs (integrating and sigma-delta). Voltage ratio calibrations to extend the operating range of an ac quantum standard therefore cannot be suitably done by applying two quantum-accurate ac voltages to calibrate the 'ac linearity' of an ADC. Alternatively, the very high performances of internal dc references currently available in top-level instruments allow sampling ac signals with a digitizer and measuring ac voltages over a wide range of values and frequencies, with the only proviso of 1% maximum distortion level of the measured signal [42]. This solution suffers from the aforementioned limitations of measurements constrained to rms voltage and will not be considered. The extreme accuracy of well known analog techniques must also be taken into account in discussing ac voltage ratio techniques. Inductive dividers were proven long ago [43] to provide accuracy at the level of few nV V<sup>-1</sup>. The high performances of inductive dividers is appealing for integration with quantum standards [44, 45], but the classical techniques are limited to pure sinusoidal signals over a limited frequency range, spanning from tens of hertz to a few kilohertz. The interest in arbitrary waveform metrology based on sampling methods with quantum traceability suggests the adoption of wide bandwidth dividers.

The suitable integration of analog and digital techniques can be considered the best way to cover all calibration ranges. The approach given here integrates quantum standards, sampling techniques and analog methods to take advantages of all these techniques. In such a method, the role of a quantum-calibrated digitizer is to sample and quantize the signal within its most accurate operating range, as shown in figure 1(b), with ordinary dividers allowing suitable up/down scaling over the whole required range. A similar approach was adopted, for instance, with dc voltage signals in [46]. Research in this field is ongoing and several solutions were proposed, that may be chosen according to specific needs or operating conditions. Two sampling voltmeters and a set of traditional dividers are integrated in a method developed within [31], where they are considered and calibrated together, with the divider connected directly to the voltmeter inputs to improve repeatability. For the even number of steps in the scaling procedure the ratio correction due to the linearity of the voltmeters can be estimated by applying the same voltage to the inputs of the voltmeters. Both step-up and step-down scaling is feasible with this method. In figure 3, the results of ac voltage calibrations using scaling up are compared to those calibrated directly against the ac-dc transfer standard. An uncertainty of the order of  $20~\mu V~V^{-1}$  up to 1~kHz at 220~V can be achieved which can be reduced to a few  $\mu V~V^{-1}$  if the scaling procedure is applied directly to the JVS and the voltage coefficients of the dividers are characterized more accurately. In designing the divider in this setup care must be taken to keep low temperature, voltage and power coefficients. An alternative solution to minimize loading effects on the voltage divider has been demonstrated in [47]. It is based on a new prototype divider that uses the split guard technique along with a buffer amplifier. The technique enabled the construction of a buffer with input capacitance below 1~pF, output impedance below  $11~m\Omega$  for frequencies below 100~kHz and overall amplitude and phase transfer error below  $2~\mu V~V^{-1}$  and  $2~\mu rad$ .

As stated above, inductive voltage dividers (IVDs) are an alternative reliable tool for realizing metrology class ac voltage ratios. In this way voltages of up to 120 V can be traced to quantum voltage standards such as JAWS [48]. However, ratios of conventional dividers must be accurately determined. Pulse-driven JVSs can be employed for this work as they can generate any voltage signal with excellent accuracy. It is possible to form highly accurate ac voltage ratios in a broad frequency range with two synchronized JAWS systems [49]. At a 1:1 ratio such calibration is very similar to a direct JAWS versus JAWS comparison [50].

#### 2.5. Current shunts

Since analog-to-digital conversion operates with voltage signals, for ac current measurements it is necessary to convert current to voltage, and for that purpose traditional resistive shunts are used. The shunt is also a scaling element, since its value can be selected to produce voltages suited to the digitizer over a wide range of current values. For instance, use of four different shunts with the nominal rms currents of 1 mA, 20 mA, 200 mA and 2 A (and with nominal rms output voltages of 0.8 V, respectively) can cover the output of commercial calibrators that generate currents up to a typical value of 2.2 A. Current shunts up to 100 A are also available, making even higher scaling possible. With the approach adopted in [51, 52], it is possible to calibrate ac currents with direct traceability to a quantum voltage standard by means of a shunt resistor. The calibration procedure includes the calibration of an ac shunt by dc reference resistors, traceable to QHR, at dc current. In that measurement set-up, the AC-QVM (AC Quantum Voltmeter [53]) is used as a dc quantum voltage standard for the resistance comparisons using a 3458A as a null-detector. It was shown for example that the ratio of two resistances can be measured with a relative uncertainty of 0.2  $\mu\Omega$   $\Omega^{-1}$  for a current of 0.9 mA. Self-heating of the shunt is one problem which needs to be addressed as well. The self-heating depends on following: the type of the shunt, on the current level applied and on the measurement procedure. Therefore, when using shunts at different current levels, either in a step-up or step-down procedures it is of great importance to consider self-heating effects. After the above calibration at dc current, the resistance of the shunt is known, and it can be used for ac current measurements by using the AC-QVM, with stable results up to 1 kHz. For instance, the stability of an ac current measurement at 62.5 Hz using a Fluke A40B-10 mA ac shunt at 3.3 mA can be done within the time interval of two to five minutes with a relative uncertainty of 0.2–0.3  $\mu$ A A $^{-1}$  (providing that the measured source is very stable and synchronized to AC-QVM). Thus, it was demonstrated that by optimizing ac current measurements procedures and using AC-QVM, it is possible to obtain accurate results within short measurement durations with direct traceability to quantum voltage standards.

## 2.6. Sampling and data analysis software

While older analog methods were usable without any computer processing, modern digital methods require vast usage of software, automation and data processing algorithms. Several applications have been developed by ADC chips manufacturers, measurement devices manufacturers, users or NMIs. Generally these applications do not deal with uncertainties.

A common situation in the data processing of sampled signals is the estimation of multiple quantities using the same record. The user is interested in amplitude and phase of the main signal component, in a spectrum, and stability of these quantities during multiple records. For the case of evaluating the properties of a digitizer, spurious free dynamic ratio, total harmonic distortion (THD) and effective number of bits are important quantities. Algorithms exists for all of these quantities, but it is complex task to learn how to use every single algorithm.

Q-Wave toolbox (QWTB) [54, 55] deals with this situation. It is an open source software toolbox written in M-code and is running in Matlab [56] or GNU Octave [57]. It aims for aggregation of high-quality algorithms required for data processing of sampled measurements. QWTB consist of data processing algorithms from different sources, unifying application interface and graphical user interface. The toolbox provides the possibility to use different data processing algorithms with one set of data and removes the need to reformat data for every particular algorithm. The Toolbox is also extensible.

The QWTB was designed to help with using general quantity estimating algorithms. However it was tailored only for simple data processing and not for actual metrological measurements with multiple hardware components and many sources of errors. Therefore, the TracePQM Wattmeter (TWM) software [58, 59] was developed. TWM is an open source, transparent, metrology grade measurement system for traceable measurement of the voltage, current, power and power quality parameters. It is designed to allow recording of the voltage and current waveforms using various digitizers and processing the measured waveforms using different algorithms. TWM defined several hardware setups and names of quantities used in QWTB. These quantities describe errors of transducers, connecting cables and digitizers. The core of TWM relies on the QWTB capabilities. An image of the user interface of the software is shown in figure 4.

The estimation of algorithm errors was not fully covered in QWTB nor in the TWM extension. Therefore a QWTB variator *QWTBvar* was developed as extension of QWTB [54]. It is

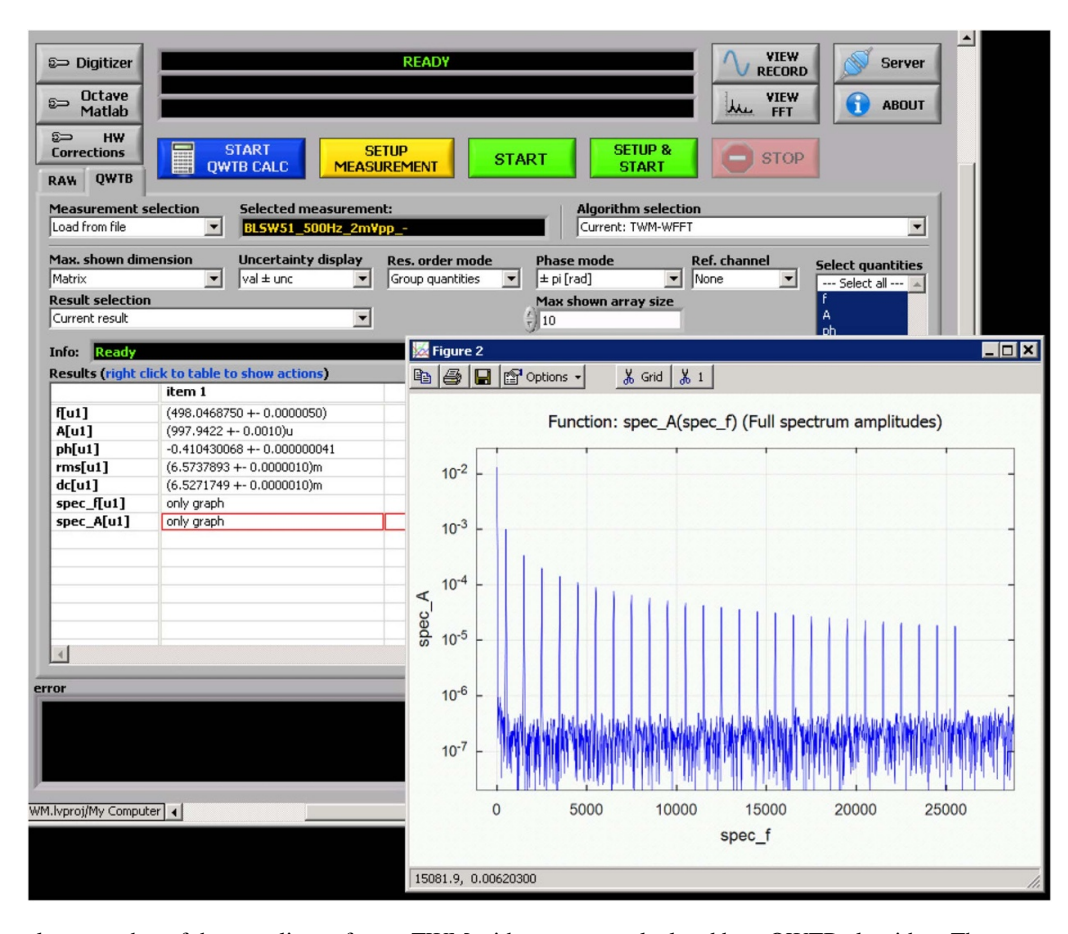


**Figure 4.** Example screenshot of the sampling software TWM with spectrum calculated by a QWTB algorithm. The source signal was a bandwidth limited square wave generated by JAWS.

a system that can easily variate input quantities or their uncertainties, calculate errors of output quantities to the nominal values, plot dependence of output quantities on the variated input quantities or their uncertainties, create a lookup table of uncertainties of output quantities and interpolate the lookup table for a quick estimation of uncertainties.

# 3. Results

Various parts of the proposed system for digital traceability were characterized and a selection of the results are presented below. In these measurements, Josephson voltage systems were used to provide precisely known stable inputs in order to characterize performance. To investigate the suitability of various digitizers for use as transfer standards, measurements were made of both the static (section 3.1) and dynamic (section 3.2) gain stability as a function of time. The target is to achieve better than 1  $\mu$ V V<sup>-1</sup> stability in gain over the time between the calibration of the digitizer against a quantum standard and its use as a transfer standard. The effect of the temperature of the digitizers on its static gain stability was also measured (section 3.1.2) to investigate the performance under different operating conditions. The combination of digitizers with current shunts to provide traceability for current measurements was investigated in section 3.3. A comparison of the proposed method against the existing thermal method was performed. Finally, a novel method using a multi-tone waveform of combined sine waves for a faster calibration method was investigated (section 3.3.2).

#### 3.1. Characterisation of static performance of digitizers

3.1.1. Static gain stability of digitizer. The static gain stability of two types of integrating digitizer was measured. Firstly, the static gain stability of the 1 V range of a 28 bit integrating digitizer (Keysight 3458A) was investigated using a 1 V PJVS system described in [21, 22]. The static gain was measured a few times per day for several days during each operation of the system. This observation was repeated at different times over more than two years. Custom developed software evaluates the quantum state (if the PJVS is within its operating margins) of the measurements as described in [21, 22]. Rapid and automatic switching ability of the PJVS between quantum voltages helps the gain measurements to be free from thermal noise and offset errors as proved in [22]. This also helps obtain sufficient measurements in a short time to observe statistics on the gain and non-linearity as shown in the data presented in [21]. The daily and long term gain stability of the digitizer was investigated for metrological purposes as shown in figure 5. The y axis of figure 5 represents the difference of static gain of the digitizer which is depicted by  $m_{400}$  ms (the static gain when the aperture time is equal to 400 ms) from

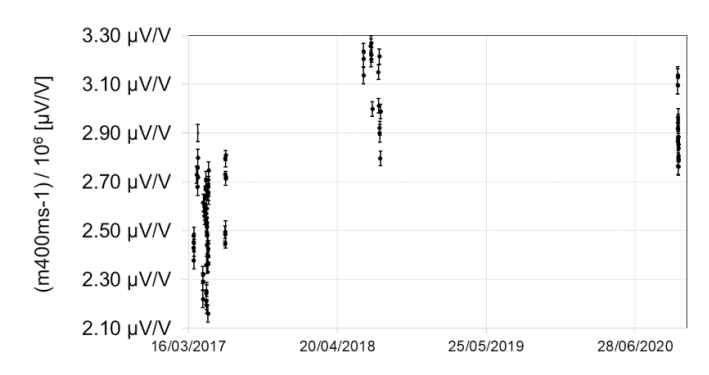


**Figure 5.** Static gain stability of an integrating digitizer as a function of time.

the ideal gain 1 V V $^{-1}$ . Daily drift of the gain of this digitizer is much less than 0.5  $\mu$ V V $^{-1}$  and the drift during an hour is less than 0.05  $\mu$ V V $^{-1}$ . The Integral Non-Linearity (INL) was also measured as described in [21, 22]. The INL was measured to be less than 0.12  $\mu$ V V $^{-1}$  even for the 1 V range of the digitizer.

Further measurements of the static gain of the Keysight 3458A were also performed with a different PJVS [9]. This PJVS system uses custom built electronics that are designed to operate at 100 kHz. The digitizer was investigated at the significantly higher sampling rates to better understand the effect on its performance. At 100 kHz (the maximum sampling rate of the DCV mode), the maximum aperture time allowed by the instrument is 1.4 µs. To trigger the digitizer at the maximum sampling rate, the EXT Trig IN socket must be used. The bias source provides a trigger signal for each generated point which was initially used to trigger the digitizer but this did not allow the aperture to be positioned in time with respect to the start of each quantized voltage step. Instead, a function generator was locked to the system master clock (provided by a 10 MHz Rubidium oscillator) and used to mimic the bias source trigger signal with a variable delay. This allowed the aperture to be aligned with the quantized voltage step. The timing of the delayed pulse can be verified using Ext Out socket from the digitizer. The delayed pulse was positioned just before the end of each 10 µs wide step and the timing was visually verified by examining the Ext Out signal on an oscilloscope. The sampling frequency of the Ext Out signal from was also verified using a counter. In conclusion, using the method described above, the quantized voltages from the PJVS were synchronized to the Keysight 3458A for sampling at the maximum sample rate of 100 kHz.

In order to measure the static gain, a triangular waveform with a frequency of 12.5 Hz at 100 kHz sampling rate, peak amplitude of 1 V and 8000 unique voltage values was used. The Keysight 3458A data was obtained using the TWM software [58] with an aperture of 1.4 µs. Two parameters (array bias trim current and trigger delay) were varied between measurements to assess their effect on the results. The array bias trim current uniformly adjusts the current driving all segments of the array and is therefore a measure of array quantization. The trigger delay shifts the position of the aperture on the step by up to 8 µs. The sampled data was analysed by

subtracting the measured voltages from the calculated voltages for each point in the waveform, generating the voltage difference curve. In addition, the static gain of the instrument was extracted from the data using a linear fit. The voltage difference results are shown in figure 6 with this gain correction applied. In figure 6(a) the five measurements show very similar results with a noise of  $\approx 200 \ \mu V \ V^{-1}$  for all curves. This is not unexpected with an aperture of 1.4 µs since at a sample rate of 100 kHz the resolution of the digitizer is significantly reduced to 16 bits and only 4.5 digits. Both trigger delay and bias trim do not effect the voltage difference curves, showing that quantized voltages were sampled. These measurement parameters were used to demonstrate the most extreme high frequency sampling scenario for the DCV function. Additionally, the error in the static gain (G-1) had a value of 240  $\mu V V^{-1} \pm 2 \mu V V^{-1}$  for all five curves, which is consistent with the fixed aperture time used for all measurements.

Measurements of static gain were also performed at a sampling frequency of 50 kHz in order to investigate the effect of the aperture time on the voltage difference curves. The same waveform was used but the timing between each generated point was doubled hence the waveform frequency reduced by half. The voltage difference curves are shown in figure 6(b). The voltage difference curves have a similar shape but the noise was reduced by half or more in comparison to the  $100 \,\mathrm{kHz}$  results shown in figure 6(a). The noise reduced as the aperture time increased. The digitizer reports the same numerical resolution at both 50 kHz and 100 kHz sample rates but the lower sample rate allows longer aperture times to be selected, leading to an improvement in the observed linearity and noise. The error in the static gain varies between the three measurements with values of  $90.0 \,\mu\text{V}\,\text{V}^{-1} \,\pm\, 0.8 \,\mu\text{V}\,\text{V}^{-1}$ ,  $60.0~\mu V~V^{-1} \pm 0.6~\mu V~V^{-1}$  and  $50.0~\mu V~V^{-1} \pm 0.5~\mu V~V^{-1}$ for 3 µs, 4.5 µs and 5.5 µs aperture times respectively. These results show that the Keysight 3458A can be operated at high sampling rates but it is important to understand how the measurements will be affected.

Secondly the temporal stability of the static gain of a different integrating digitizer (Fluke 8588A) was investigated. To estimate gain stability over time, the Allan deviation is a good measurement method [60]. The digitizer is set to sample a large amount of data and the Allan deviation is calculated for different observation periods. The results show the typical deviation of the gain after a selected time. This is especially important for measurement setups where digitizer gain is calibrated and the same digitizer is used to calibrate DUT at some later time. Allan deviation provides information on how much the gain can deviate in the time between the gain calibration and the DUT calibration. This value should be included in the uncertainty budget of the measurement.

An example of a gain stability estimation is shown in [61]. The digitizer was connected to a stable signal of approximately 10 V generated by PJVS and set to a range of 10 V. A record of 10<sup>7</sup> samples was obtained and analysed by the overlapped Allan deviation (OADEV) function [62]. Such a measurement can be done not only for the gain, but also for the case of shorted inputs to identify internal noise properties. An example of such a measurement is shown in figure 7 for the

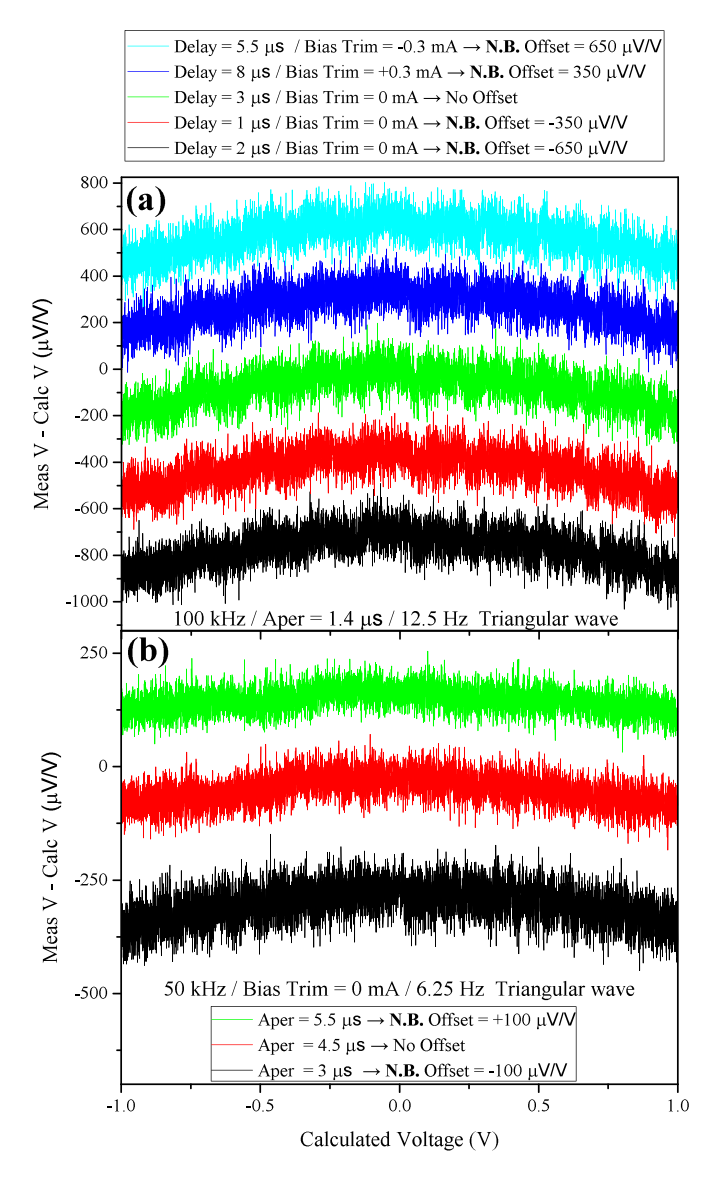


**Figure 6.** The voltage difference curves for a Keysight 3458A at sampling rates of (a) 100 kHz and (b) 50 kHz, measuring a triangular waveform of frequency (a) 12.5 Hz and (b) 6.25 Hz with a peak amplitude of 1 V. Both the bias trim current and trigger delay were varied. This figure is but B/W in print. Note that the legend order denotes the position the curves in the two graphs and the curves are offset for clarity.

range of the device set to 0.1 V and for various apertures and sampling periods. According to the specifications the minimal value of aperture setting is 0 ns, which means the analog value is held at 0 ns, the time the trigger occurs. Aperture settings other than 0 ns use an averaging algorithm (see [63], page 40). The figure reveals that averaging up to 0.03 s helps to decrease type A uncertainty. However for apertures 0.2 µs and longer the drift of the offset starts to be important.

3.1.2. Static gain thermal drift. The temperature influence on the frequency response of Keysight 3458A digitizers in DCV sampling mode has been studied in [64] for dc voltage references and in [65] for ac input signals up to 1 kHz.

Results show a similar behaviour for both dc and ac signals, with two very well differentiated behaviours of the temperature coefficient when aperture time is higher and lower than 100 µs. This behaviour is a consequence of the ADC switching between  $10\,\mathrm{k}\Omega$  and  $50\,\mathrm{k}\Omega$  inputs at  $100\,\mathrm{\mu}s$ . For high integration times ( $T_a > 100\,\mathrm{\mu}s$ ) the temperature influence is negligible (0.5 µV V $^{-1}$  °C $^{-1}$ ) whereas at low integration times ( $T_a < 100\,\mathrm{\mu}s$ ) the temperature influence is important (3 µV V $^{-1}$  °C $^{-1}$  to 7 µV V $^{-1}$  °C $^{-1}$ ), depending on digitizer and aperture time), and it should be characterized for each digitizer when the measurement temperature is different from the digitizer calibration temperature.

## 3.2. Characterisation of dynamic performance of digitizers

3.2.1. Dynamic gain stability and linearity. The NI5922 digitizer was characterized using a JAWS for both short and long term dynamic gain stability as well as the linearity of the response to the input ac waveform. Firstly, a set of JAWS waveforms with 80 mV amplitude (7500 Josephson junctions operated at 14.1 GHz) as described in section 2.1.2 were applied. Well-quantized sine waves within the frequency range from 1 kHz to 100 kHz were directly applied to the digitizer. The digitizer was synchronized and triggered by the JAWS, and set to the 2 V range, 1 M $\Omega$  input impedance, standard 48-tap FIR filter. 40 000 sine wave periods were measured using a sampling rate of 4 MSa s $^{-1}$ .

All data were averaged to one period as shown in figure 8. The measured deviation from the JAWS input sine (red curve in figure 8) shows a specific 'pattern' which remains independent of frequency and deviations from the nominal value vary within  $\pm 7 \,\mu\text{V} \,\text{V}^{-1}$ , but can be as large as 13  $\mu\text{V} \,\text{V}^{-1}$ . We note that the spikes around maximum amplitudes are present after averaging 40 000 periods i.e. they are not caused by spurious jumps but are in fact a non-linearity existing in the sampler. We also investigated the long term gain stability of the digitizer by running an overnight measurement. The setting of the sampler was the same as for the previous experiment. The JAWS sine wave frequency was set to 100 kHz and measured with the sampler for 15 h. It is expected that the JAWS output does not change with time [50]. Figure 9 shows the result for such a measurement. The gain variation with just five seconds integration time varies within  $\pm 15~\mu V\,V^{-1}$  over the time of the exercise. A linear gain drift of  $-0.53 \mu V V^{-1}$  per h is visible. For a 1 h integration time (blue line in figure 9) deviations to the linear drift line are typically within 2  $\mu$ V V<sup>-1</sup>. This is consistent with an Allan deviation analysis similar to the one shown in figure 10. All deviations are substantially within the specifications of the instrument [66]. Furthermore, the digitizer is very well suited for differential measurements in an AC quantum voltmeter [67]. However, both investigations show that sampler has a limited linearity and stability. A careful linearity correction and hourly Josephson-based re-calibration are required for scaling applications aiming at the  $\mu V V^{-1}$ level.

The dynamic gain stability can also be estimated using the Allan Deviation. Such a method was shown in [28]. An ac signal was generated by JAWS and applied to a National

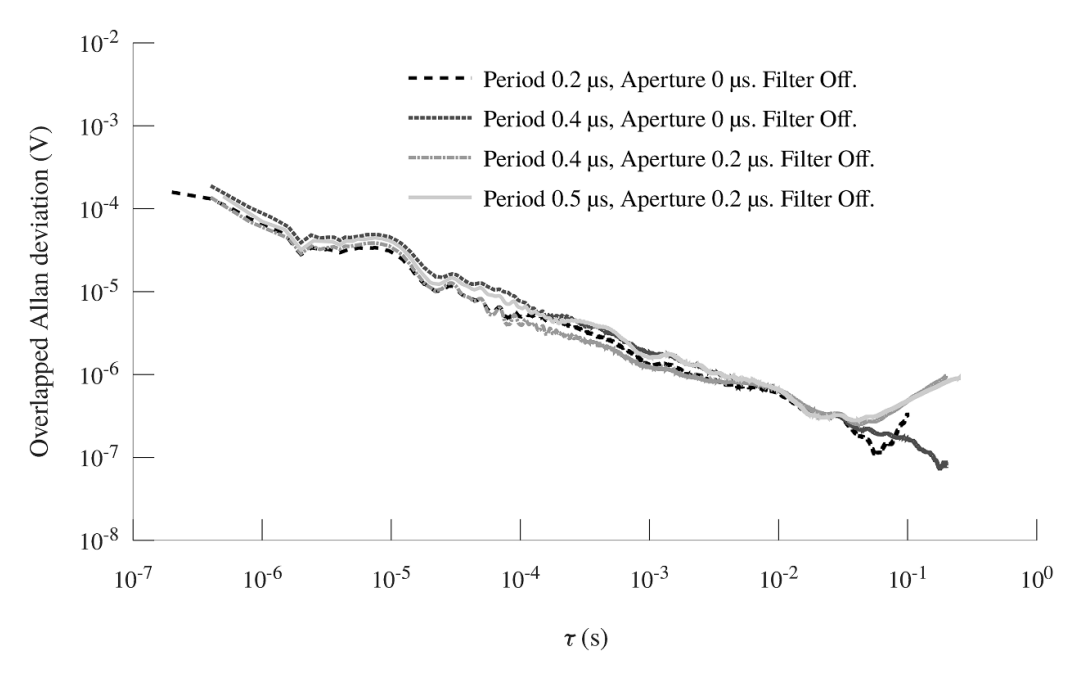
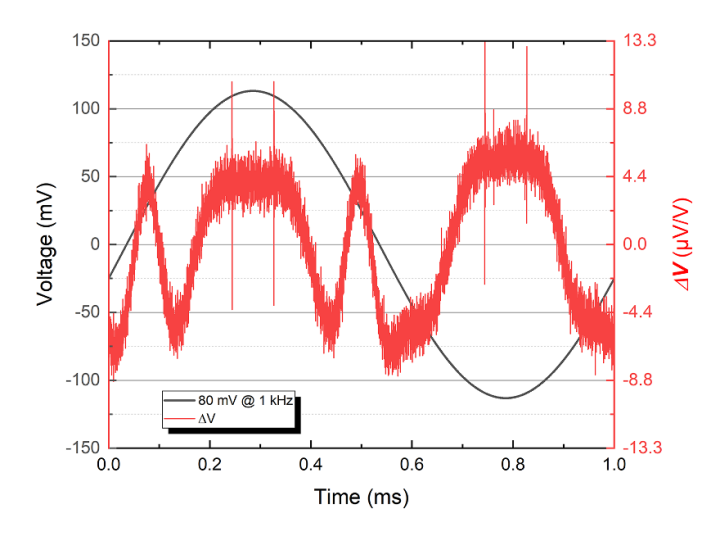
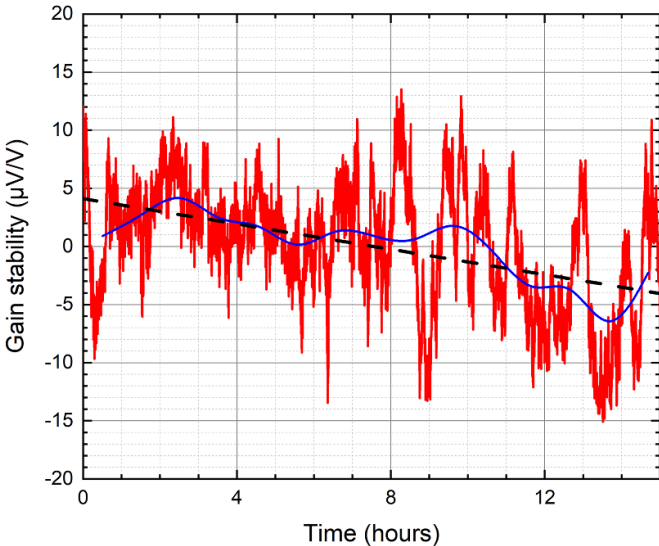


Figure 7. Dependence of overlapped Allan deviation on observation time  $\tau$  for digitizer Fluke 8588A set to range 0.1 V with shorted input. Results for four settings of the multimeter aperture and sampling periods are shown. An aperture time of 0  $\mu$ s refers to the instrument minimum aperture setting where the value is held at the time the trigger occurs.



**Figure 8.** Linearity measurement of an 80 mV sine wave at 1 kHz (black line, left axis). The red curve shows deviations from this sine wave, right axis.

Instruments 5922 digitizer. The signal was divided into a number of sections and processed by amplitude estimating algorithms. The calculated amplitude was further process by the OADEV algorithm. Due to highly stable properties of JAWS, all measured stability can be accredited to the digitizer and the amplitude estimating algorithm. Multiple of these algorithms have been used to demonstrate that the measured stability was inherent to the digitizer. The results show the stability of the digitizer for various time periods, this time for an ac signal of selected frequency or amplitude. Figure 10 shows such a measurement for signals of frequency 150 Hz and amplitudes from  $\approx 0.092$  V to  $\approx 0.646$  V. One can see that for time



**Figure 9.** Long-term gain stability measurement of the NI5922 for an 80 mV JAWS sine wave at  $100\,\mathrm{kHz}$ . The red and blue lines correspond to a 5 s and a 1 h integration time, respectively. The dashed black line indicates a long-term linear drift of about  $-0.53~\mu\mathrm{V}~\mathrm{V}^{-1}$  per hour.

periods longer than  $\approx 10$  s the drift is dominant over the random noise of the digitizer gain.

# 3.3. Characterisation of complete system

3.3.1. Characterization of digitizer with current shunt. In the new digital method for current and voltage traceability (as shown in figure 1(b)), TVCs are replaced by digitizers. In this

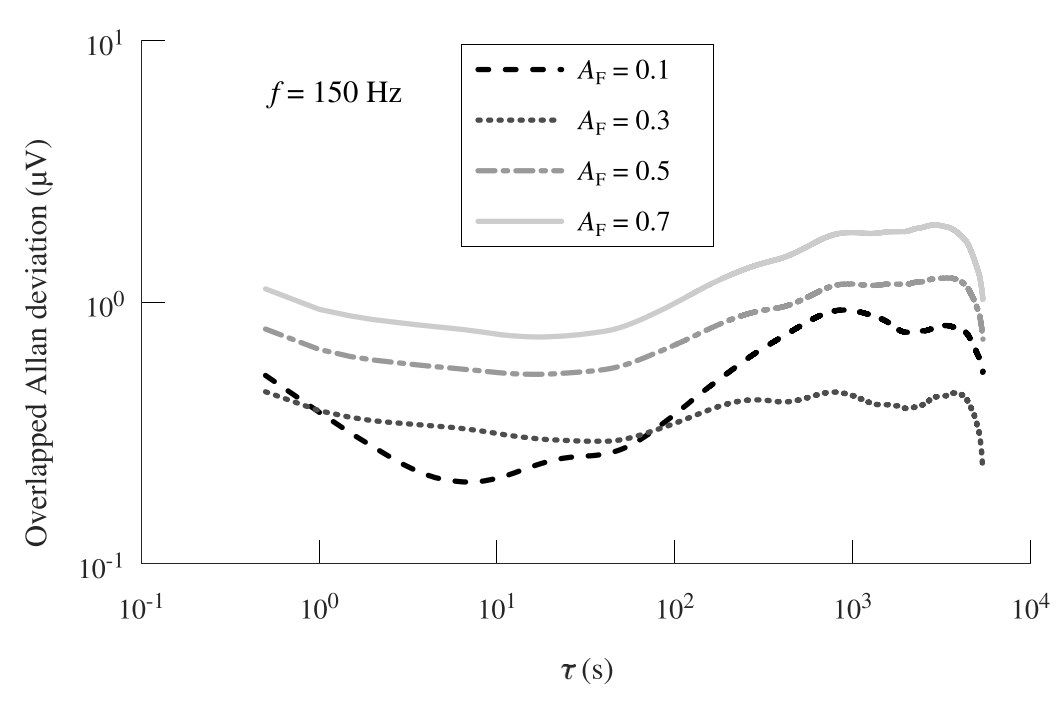
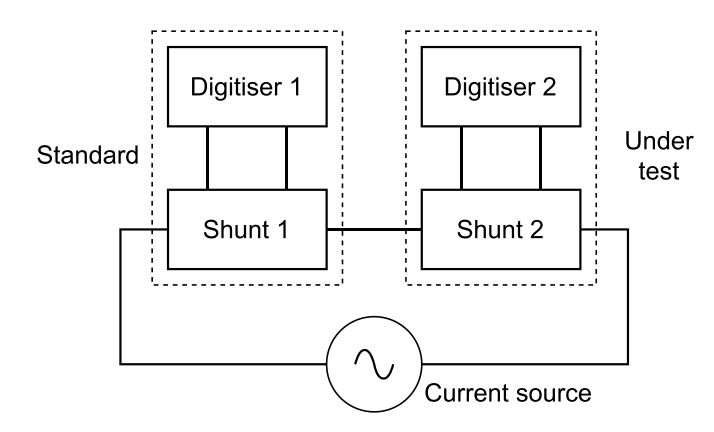


Figure 10. Dependence of Overlapped Allan deviation on observation time  $\tau$  for digitizer National Instruments 5922 set to 1 V range. Results for four signals of amplitudes:  $\approx 0.092$  V ( $A_F = 0.1$ ),  $\approx 0.277$  V ( $A_F = 0.3$ ),  $\approx 0.461$  V ( $A_F = 0.5$ ), and  $\approx 0.646$  V ( $A_F = 0.7$ ).



**Figure 11.** Setup of the new digital current step-up. The standard shunt-digitizer is calibrated against Josephson voltage standard. Then the digitizers output is compared and the correction required for the shunt-digitizer under test is calculated. The complete digital traceability chain is established by repeating the process for higher currents.

way, a current source provides the same current to two combinations of shunt-digitizer; the shunt-digitizer under test and the standard shunt-digitizer, as shown in figure 11. By comparison of the digitizers output and knowing the correction of the combination standard shunt-digitizer (by characterization against a JVS), the correction of the shunt-digitizer under test can be calculated. By repeating this process for higher currents, a complete digital traceability chain can be established.

This new method and an initial validation is described in [68]. Two digitizers (both Keysight 3458A) were used to step-up from 20 mA to 1 A in five steps. Nine frequencies, from 10 Hz to 10 kHz and dc were considered. The validation

consisted of the comparison of the shunt ac-dc difference obtained by thermal and digital methods. In this comparison dc measurements were performed because the traditional TVC approach provides just the ac-dc difference. Nevertheless, in a digital-based current step-up, dc measurements are not necessary. The comparison of both methods can only be based on the ac-dc difference of the shunts alone. Therefore the influence of the TVC and digitizers had to be eliminated from the measurements. In the thermal converter method it is assumed that the ac-dc difference of the shunt and TVC combination adds arithmetically. The ac-dc difference of the TVC is known. To eliminate the digitizer influence in the digital method, two sets of measurement were performed, one with the setup shown in figure 11 and another swapping digitizers. The combination of these two measurements allowed the elimination of the digitizers influence and the comparison of the two methods. Results in [68] show that up to 1 kHz the difference between both techniques is very small ( $<2 \mu A A^{-1}$  at 1 kHz).

3.3.2. Multi-tone calibration waveforms. A quantum validation of the digital step-up technique described in section 3.3.1 was performed. Two digitizers (Keysight 3458A) were used together with two shunts of 20 mA and 50 mA. Three signals with three different frequencies (100 Hz, 400 Hz and 1 kHz) were input and combined allowing the analysis of dynamic signals. The combinations included the same amplitude/same phase, different amplitude/same phase, and same amplitude/different phase. An example is shown in figure 12, where three waveforms with the same amplitude and phase are combined to generate a multi-tone input. The quantum validation was divided into three phases as indicated in figure 13. In

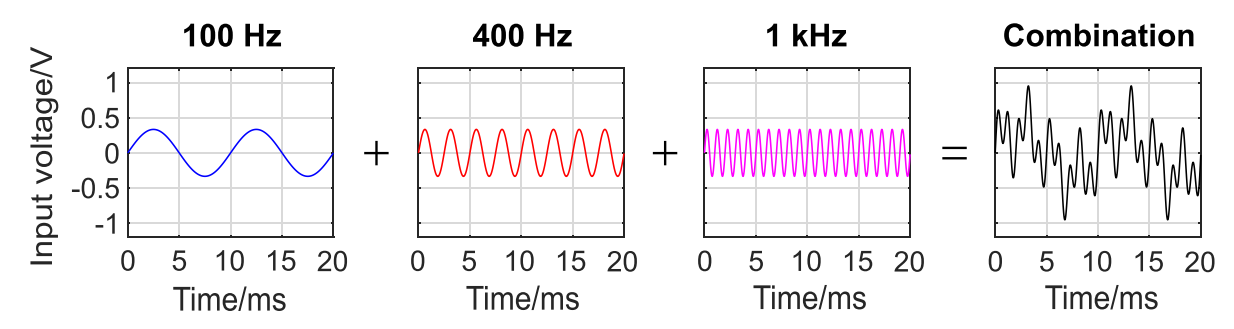


**Figure 12.** Combination of three simple waveforms with different frequencies (100 Hz, 400 Hz and 1 kHz), of the same amplitude and same phase. The resulting multi-tone signal is used to validate the digital step-up technique against dynamic signals.

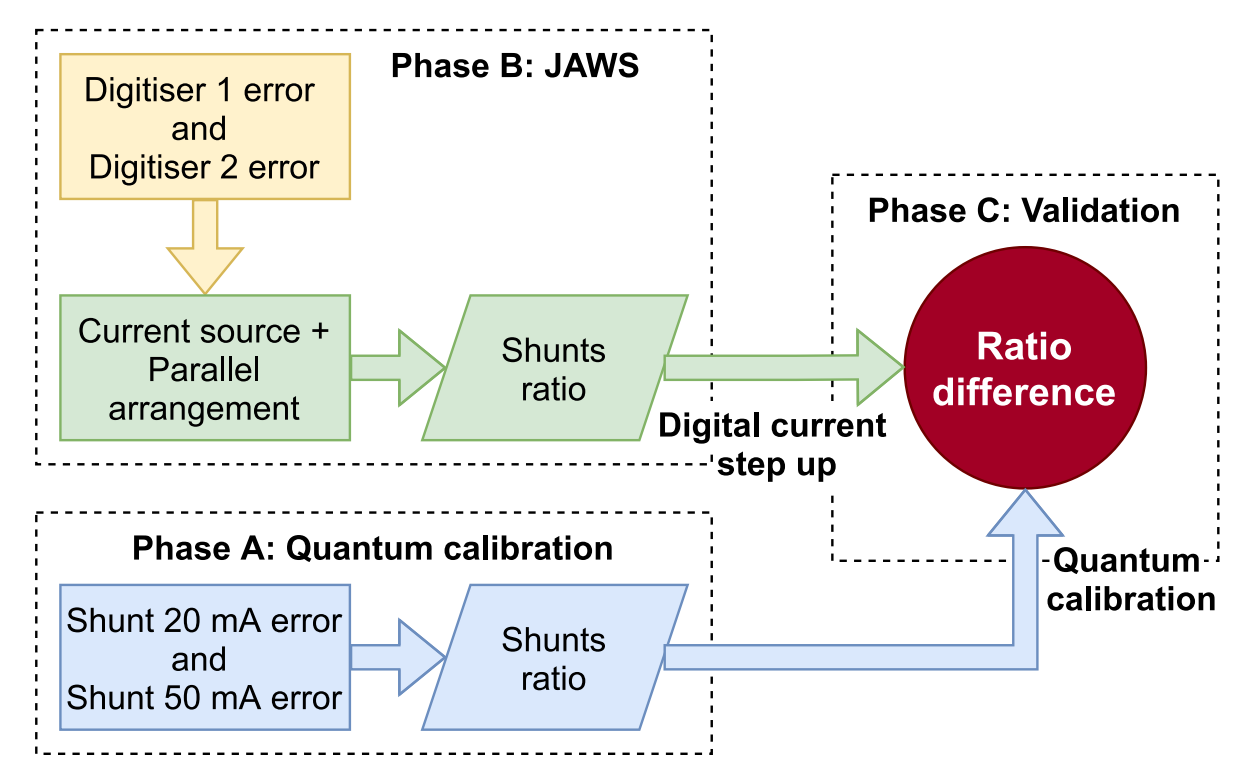


**Figure 13.** Quantum validation of digital current step-up. In phase A the quantum calibration of shunts is performed. In phase B digitizers are calibrated against JAWS. In phase C the corrected shunts ratio is compared to shunts ratio from quantum calibration.

phase A, the quantum calibration of the shunts was performed as explained in section 2.5, resulting in the determination of shunts resistance with an uncertainty in the sub  $\mu V V^{-1}$  range. In phase B, digitizers were characterized against JAWS, calculating the correction necessary for each singled or combined signal, frequency and digitizer. Finally, in phase C, the validation is performed by comparing the shunts ratio after digitizer output correction using the setup shown in figure 11 and the ratio from quantum calibration.

Results showed that the ratio difference obtained by quantum calibration and the step-up method after digitizer correction is in the order of few  $\mu V V^{-1}$ , validating the new digital method for traceability of current. This allows high accuracy dissemination for complex waveforms that vary with time or have a significant amount of harmonic content and at the same time provides calibration procedures that are simpler and shorter. Further details and results will be included in an article in preparation [69].

## 4. Uncertainties

Uncertainties of quantities estimated from sampled data are based on the following uncertainties of input quantities:

- (a) type A uncertainty,
- (b) type B uncertainties estimated from hardware,
- (c) type B uncertainties caused by a data processing.

The first type of uncertainty, type A, is caused by external or internal sources that cannot be repeated and quantified in other ways than by statistical means. Type A uncertainty is estimated by repeating the measurements which can usually be performed by any available sampling software. The second and third type of uncertainty, type B, is the *prior knowledge*. Any hardware used in the measurement setup increases the uncertainty of measurement, such as transducers, transmission

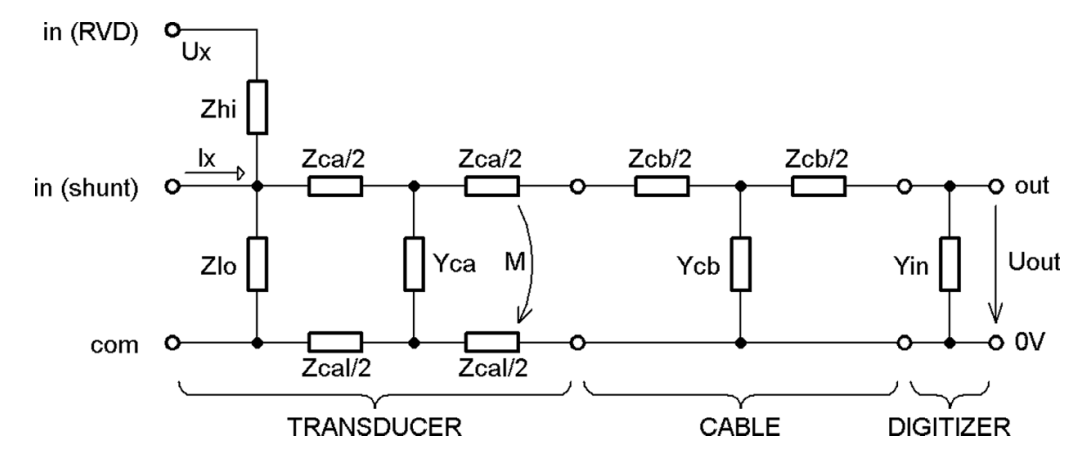


Figure 14. TWM correction design for single ended direct connection measurement. Impedance values (Z, Y) and their uncertainties for transducer, cable and digitizer can be used to calculate correct value and uncertainty of estimated quantities. More complex designs are available.

cables, digitizers, and signal sources. Calibration data, correction coefficients and the related uncertainties of measurement elements have to be known to successfully estimate output quantities and their uncertainties. Both types of uncertainties are extensively described in the existing literature [70–72].

The third type of uncertainty, caused by imperfections of quantity estimating algorithms, are very hard to estimate and not yet sufficiently described in the literature. A basic description can be found in [73]. Example of algorithms errors can be found in [74]. Various algorithms return different results for the same input data due to different underlying calculation methods. It is very hard to discover the errors of the algorithm for the actual measurement. One has to know all errors and sources of uncertainties to obtain the value of the algorithm error. However there are at least two unknown source of errors during a calibration of a DUT: the DUT itself and the algorithm. Therefore simulations are used to estimate algorithm errors, e.g. [75]. Simulation provides the possibility to control errors and input uncertainties to find out the error of the algorithm. Based on the simulation, an uncertainty can be assigned to the algorithm and used in the real measurements. Unfortunately, simulation cannot cover all the details of a real measurement.

The propagation of type B uncertainties is carried out using using GUM Uncertainty Framework (GUF) [70] or Monte Carlo Method (MCM) [71, 72]. Yet using both methods is very complex as the sampling measurement methods use a large amount of data and implements numerous sources of uncertainties.

QWTB was developed with the aim of easy uncertainty propagation, and TWM was developed to use these qualities for actual sampling measurements. Calibration data of the measurement setup can be loaded into the TWM system and the algorithm can use it for evaluation of the output uncertainty. TWM can cover many corrections and uncertainties for the whole measurement chain from transducer, connecting cable to digitizer. Figure 14 shows the basic correction design for a single ended direct connection measurement. Quantities  $Z_{\rm hi}$  and  $Z_{\rm lo}$  describe high and low impedance of a resistive voltage divider or impedance of a shunt. Quantities  $Z_{\rm ca}$  and

 $Y_{\rm ca}$  describe impedance and admittance of the transducer output terminals. Quantities  $Z_{\rm cb}$  and  $Y_{\rm cb}$  describe impedance and admittance of the cable connecting the transducer to the digitizer. M is mutual inductance in the system.  $Y_{\rm in}$  is an input admittance of the digitizer. By assigning the values and their uncertainties, the values calculated by QWTB algorithms are corrected for the transducer scaling and transducer loading effects. Other correction configurations including buffer, differential connection or combinations are available, as detailed comprehensively in [76]. Several algorithms have been extended to utilize the corrections and uncertainties.

# 4.1. Example of algorithm validation

Quantum systems are suitable for finding algorithm errors due to the ability to generate signals with known values. Yet the DUT can still cause unknown errors and it is difficult to establish if the source of the error is part of the DUT or the data estimation algorithm. The following method can be used to characterize the performance of the algorithm. One can artificially limit the measured data and examine the performance of the algorithm. An example of this method is shown in the following example testing the validity of uncertainties estimated by the algorithm calculating THD.

Algorithm TWM-THD with uncertainty estimation was validated in [77]. The algorithm is capable of estimating the uncertainty and using multiple records to estimate the influence of the noise. Multiple records are used to perform averaging of complex values of DFT (discrete Fourier transform) outputs, and the averaged spectra are used to estimate noise level and value of THD. Thus it is not a simple average of THD values, but an averaging of noise in the complex plane of the Fourier transformation. The algorithm partly use MCM, therefore it is not possible to build an uncertainty budget. Based on simulations, the performance of the algorithm increases with increasing averaging and length of the records.

To test validity of the uncertainty estimation, a sine wave signal of frequency 4.8 kHz and amplitude 25 mV has been generated by the JAWS system. The digitizer sampling frequency was set to 480 kHz. The digitizer sampling was

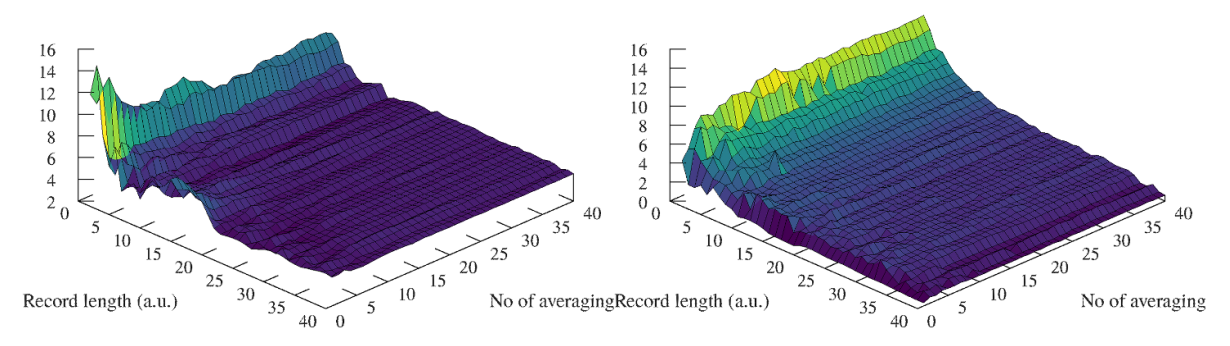


**Figure 15.** THD value (left) and uncertainty (right) as calculated from record of various lengths and number of averaging. The record length is expressed as multiple of 40 signal periods. Values of THD and uncertainty are multiplied by  $1 \times 10^6$ .

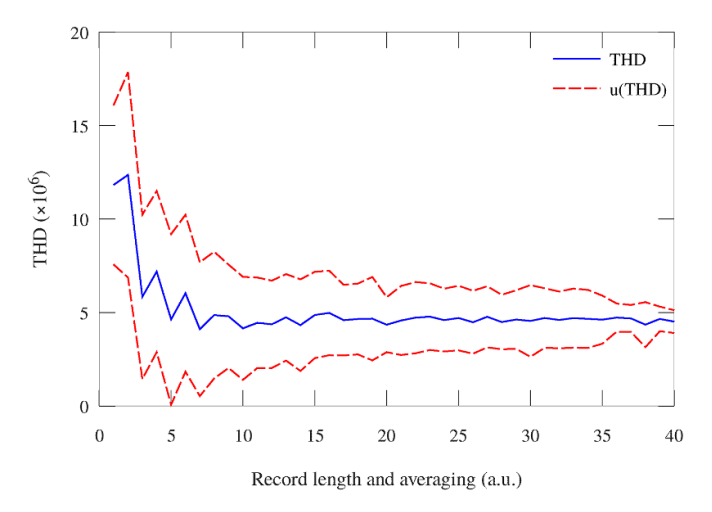


**Figure 16.** THD value and its uncertainty for increasing record length and number of averaging. Line graph represents diagonal cross-section of graphs shown in figure 15.

coherent to the signal source. A waveform of 10<sup>6</sup> samples has been recorded. The records have been split into multiple sections of the same length. The THD was calculated for various number of sections (increased complex averaging) and various number of samples in the sections. Based on the simulation, the value calculated from the highest number of longest sections is the most probable value. However even for smaller number of sections of shorter length the THD uncertainty should be correctly estimated by the algorithm.

The resulting THD and its uncertainty is shown in figure 15. The plots cover the span of averaging from 1 (no averaging) to average from 40 records, and the record length span is from Section of 40 signal periods (4000 samples) to section of 1600 signal periods ( $160 \times 10^3$  samples).

The record length is expressed as multiples of 40 signal periods. The THD value tends towards a value of  $4.6 \times 10^{-6}$  with increasing number of averaging and increasing length of record. The uncertainty behaves similarly and tends towards to a value of  $0.61 \times 10^{-6}$ . For clarity, figure 16 shows only the value from the diagonal of the previous figure. One can see all but first two values of calculated THD uncertainties encompass the most probable value for highest number of sections and longest records showing that the uncertainty

estimation of the algorithm was correct for the majority of the results.

#### 5. Conclusion

We propose a new method for providing traceability to the SI for ac voltage and current. This method is based on the utilization of Josephson voltage systems, both PJVS and JAWS to characterize high performance digitizers. When used with voltage dividers and current shunts, these digitizers can provide a more direct traceability chain having the advantages of reduced measurement time as well as reduced hardware requirements. Increased data processing capability is required, however this can be automated. The use of sampling allows the spectral content of the waveforms under test to be evaluated which is not possible in thermal-based methods. The hardware components required for this proposed new method should be selected on an individual basis depending on the application as well as the available facilities and the availability of individual components. We described some commonly available systems and instruments typically found at NMIs and presented various results of the characterization of these components

An approach combining traditional scaling methods with the use of a digitizer operating within its optimum operating range was adopted to extend the traceability range. In this way the digitizer, fully characterized against a Josephson standard, operates in the quantum calibrated range and the divider section extends the scale of values directly traceable to the standard. The use of resistive and IVDs for voltage scaling were investigated as well as the use of current shunts. Resistive dividers are particularly interesting, owing to their wide bandwidth and ease of integration with digital instrumentation; they allow scaling of voltages down to 10 mV and up to 220 V for signals with maximum frequency of 5 kHz. The current shunts allow scaling of currents from 1 mA up to 100 A, for the frequencies of interest up to 1 kHz (but also well above, up to 100 kHz). It was shown that their dc resistance can be determined using AC-QVM with an uncertainty of 0.1  $\mu\Omega\Omega^{-1}$ , while using the same system at ac enables current measurements with an uncertainty of  $0.3 \mu A A^{-1}$ , with the optimised measurement set-up and procedures. Both enables direct traceability route to the quantum standards.

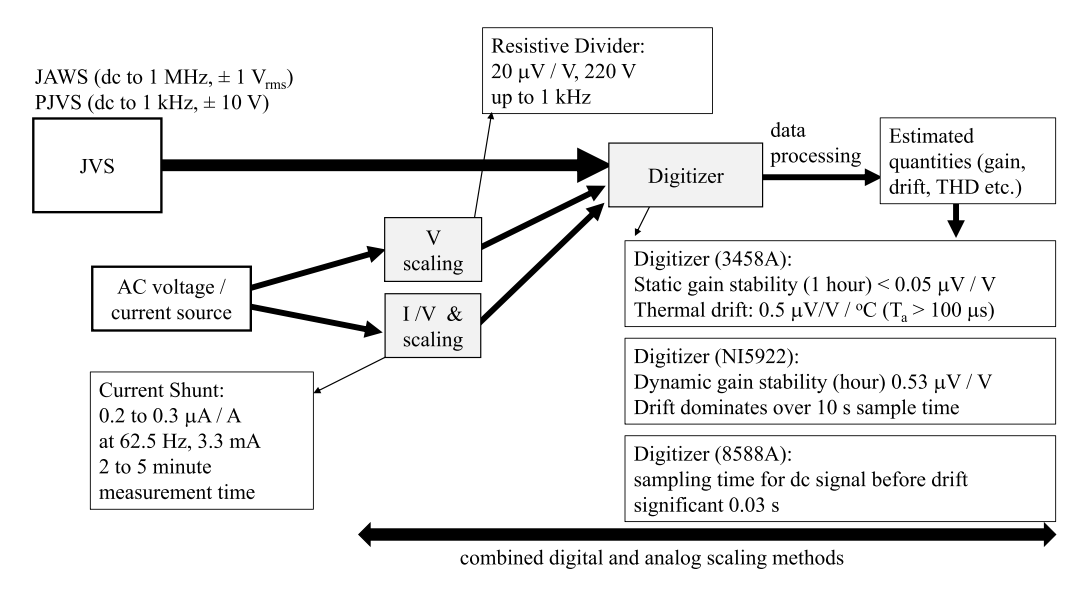


**Figure 17.** Summary of characterization of components of the proposed traceability chain. The results shown indicate performance under certain selected operating regimes and represent best achievable performance.

Measurements of the static gain stability of the Keysight 3458A have shown long term stability suitable for use as a transfer standard. Use of this digitizer to sample at PJVS waveform at the maximum sample frequency of 100 kHz has been demonstrated. The effect of temperature on this instrument has been found to be significant only below 100 µs aperture time where correction must be made if using the instrument at a different temperature. The Fluke 8588A has shown gain stability that reaches an optimum at around 0.03 s sample time. The dynamic performance of the NI5922 has revealed a larger variation in gain, up to 25  $\mu$ V V<sup>-1</sup> for a few minutes integration time. To make it suitable for use as a transfer standard two parameter must be mastered. Firstly, the integration time needs to be increased e.g. to one hour and the gain drift needs to be compensated by regular Josephson-based calibrations. Secondly, the non-linearity of the device needs to be measured and compensated which is challenging but possible.

Traceability for current measurements using a digitizer and current shunt characterized as a single unit has shown good agreement with thermal methods. This shows sufficient performance for use in addition to thermal methods at frequencies up to 1 kHz. Initial study of the use of multi-tone waveforms shows promising potential for further reducing measurement time via the application of several frequencies at once with no loss of accuracy. The use of complex waveforms is very useful for analysis of dynamic measurements.

Uncertainty analysis methods have been developed to accommodate the non-ideal performance of system components. An example of the use of this method to measure THD has shown that this analysis method is a valid and useful tool for determining the measurement time required to achieve lowest uncertainty, reducing the use of unnecessarily long measurements which do not reduce the uncertainty past the limiting value.

In summary, the initial characterization measurements and investigation of a new digital traceability chain for ac voltage and current have shown promising results and it is expected that future work will involve the integration of these digital methods into NMI traceability chains and will, in the longer term, replace thermal-based methods.

# Data availability statement

The data that support the findings of this study are available upon reasonable request from the authors.

# **Acknowledgments**

This work was co-financed by the EMPIR joint research Project 17RPT03 DIG-AC [31]. The EMPIR programme is co-financed by the Participating States and from the European Union's Horizon 2020 research and innovation programme.

# **ORCID iDs**

J Ireland https://orcid.org/0000-0002-2563-3854

M Šíra https://orcid.org/0000-0002-9322-5991

S Mašláň https://orcid.org/0000-0002-8536-9119

R Behr https://orcid.org/0000-0002-5480-443X

D Ilić https://orcid.org/0000-0003-4816-8091

#### References

- [1] JCGM 2019 The International System of Units (SI Brochure (EN)) 9th edn (Paris: Bureau International des Poids et Measures)
- [2] BIPM-CCEM 2019 Mise en pratique for the definition of the ampere and other electric units in the SI (Paris: Bureau International des Poids et Measures)
- [3] BIPM KCDB database (available at: www.bipm.org/kcdb/)

- [4] Williams E S 1971 Thermal voltage converters and comparator for very accurate ac voltage measurements J. Res. Natl Bur. Stand. C 75C 145–54
- [5] Inglis B D 1992 Standards for AC–DC transfer *Metrologia* **29** 191–9
- [6] Budovsky I, Georgakopoulos D, Hagen T, Sasaki H and Yamamori H 2011 Precision AC–DC difference measurement system based on a programmable Josephson voltage standard *IEEE Trans. Instrum. Meas.* 60 2439–44
- [7] Rüfenacht A, Flowers-Jacobs N E and Benz S P 2018 Impact of the latest generation of Josephson voltage standards in ac and dc electric metrology *Metrologia* 55 S152–73
- [8] Kohlmann J, Behr R and Funck T 2003 Josephson voltage standards Meas. Sci. Technol. 14 1216–28
- [9] Williams J, Henderson D, Pickering J, Behr R, Müller F and Scheibenreiter P 2011 Quantum-referenced voltage waveform synthesiser *IET Sci. Meas. Technol.* 5 163–74
- [10] Benz S P and Hamilton C A 1996 A pulse-driven programmable Josephson voltage standard *Appl. Phys. Lett.* 68 3171–3
- [11] Lapuh R 2018 Sampling with 3458A (Ljubljana: Left Right)
- [12] Konjevod J, Malarić R, Mostarac P and Jurčević M 2021 The AC amplitude measurement characteristics of high-resolution digitizers based on calibration with thermal voltage converter and swerlein algorithm 2021 IEEE Int.

  Instrumentation and Measurement Technology Conf.
  (12MTC) pp 1–5
- [13] Konjevod J, Malarić R, Jurčević M, Mostarac P and Dadić M 2020 Comparison of digitizers for high-precision sampling power meters *IEEE Trans. Instrum. Meas.* 69 3719–28
- [14] Wijayasundara G, Kim M S, Park S N and Lee H K 2018 Calibration of AC voltage for a high speed sampling ADC board using thermal voltage converters 2018 Conf. on Precision Electromagnetic Measurements (CPEM 2018) pp 1–2
- [15] Amagai Y, Maruyama M and Fujiki H 2013 Low-frequency characterization in thermal converters using AC-programmable Josephson voltage standard system *IEEE Trans. Instrum. Meas.* 62 1621–6
- [16] van den Brom H E, Kieler O F O, Bauer S and Houtzager E 2017 AC–DC calibrations with a pulse-driven AC Josephson voltage standard operated in a small cryostat IEEE Trans. Instrum. Meas. 66 1391–6
- [17] Overney F, Rufenacht A, Braun J P, Jeanneret B and Wright P S 2011 Characterization of metrological grade analog-to-digital converters using a programmable Josephson voltage standard *IEEE Trans. Instrum. Meas.* 60 2172–7
- [18] Kim M S, Cho H, Chayramy R and Solve S 2020 Measurement configurations for differential sampling of ac waveforms based on a programmable Josephson voltage standard: effects of sampler bandwidth on the measurements *Metrologia* 57 065020
- [19] Kurten W, Mohns E, Behr R, Williams J, Patel P, Ramm G and Bachmair H 2005 Characterization of a high-resolution analog-to-digital converter with a Josephson AC voltage source *IEEE Trans. Instrum. Meas.* 54 649–52
- [20] Henderson D, Williams J M and Yamada T 2012 Application of a Josephson quantum voltage source to the measurement of microsecond timescale settling time on the Agilent 3458A 8½ digit voltmeter *Meas. Sci. Technol.* 23 124006
- [21] Öztürk T C, Ertürk S, Tangel A and Arifoviç M 2020 Using programmable Josephson voltage standard for static and dynamic gain characterization of integrating ADC *IEEE Trans. Instrum. Meas.* **69** 4425–35

- [22] Öztürk T C, Ertürk S, Tangel A, Arifoviç M and Turhan S 2017 Metrological measurements using programmable Josephson voltage standard 2017 10th Int. Conf. on Electrical and Electronics Engineering (ELECO) (Bursa, Turkey, 2017) pp 1117–21
- [23] Kim M S, Cho H and Solve S 2022 Differential sampling of AC waveforms based on a programmable Josephson voltage standard using a high-precision sampler *Metrologia* 59 015006
- [24] Palafox L, Ramm G, Behr R, Kurten Ihlenfeld W G and Moser H 2007 Primary AC power standard based on programmable Josephson junction arrays *IEEE Trans*. *Instrum. Meas.* 56 534–7
- [25] Waltrip B C, Nelson T L, Berilla M, Flowers-Jacobs N E and Dresselhaus P D 2021 Comparison of AC power referenced to either PJVS or JAWS IEEE Trans. Instrum. Meas. 70 1–6
- [26] EMPIR Joint Research Project 19RPT01 2020–2023 Quantum power—quantum traceability for AC power standards (available at: https://quantumpower.cmi.cz)
- [27] Rietveld G, Zhao D, Kramer C, Houtzager E, Kristensen O, de Leffe C and Lippert T 2011 Characterization of a wideband digitizer for power measurements up to 1 MHz IEEE Trans. Instrum. Meas. 60 2195–201
- [28] Šíra M, Kieler O and Behr R 2019 A novel method for calibration of ADC using JAWS IEEE Trans. Instrum. Meas. 68 2091–9
- [29] Lapuh R, Voljč B, Lindič M and Kieler O F O 2017 Keysight 3458A noise performance in DCV sampling mode *IEEE Trans. Instrum. Meas.* 66 1089–94
- [30] de Aguilar J D, Salinas J R, Kieler O, Caballero R, Behr R, Sanmamed Y A and Méndez A 2019 Characterization of an analog-to-digital converter frequency response by a Josephson arbitrary waveform synthesizer *Meas. Sci. Technol.* 30 035006
- [31] EMPIR Joint Research Project 17RPT03 DIG-AC 2018–2022 A digital traceability chain for AC voltage and current (available at: https://digac.gum.gov.pl/)
- [32] Öztürk T C, Ertürk S, Tangel A and Arifoviç M Using programmable Josephson voltage standard for static and dynamic gain characterization of integrating ADC IEEE Trans. Instrum. Meas. 69 4425–35
- [33] Lee J, Behr R, Palafox L, Katkov A, Schubert M, Starkloff M and Boeck A C 2013 An ac quantum voltmeter based on a 10 V programmable Josephson array *Metrologia* 50 612–22
- [34] Watanabe M, Dresselhaus P and Benz S 2006 Resonance-free low-pass filters for the AC Josephson voltage standard *IEEE Trans. Appl. Supercond.* 16 49–53
- [35] Kieler O F, Iuzzolino R and Kohlmann J 2009 Sub-μm SNS Josephson junction arrays for the Josephson arbitrary waveform synthesizer *IEEE Trans. Appl. Supercond.* 19 230–3
- [36] Flowers-Jacobs N E, Rüfenacht A, Fox A E, Dresselhaus P D and Benz S P 2020 Calibration of an AC voltage source using a Josephson arbitrary waveform synthesizer at 4 V 2020 Conf. on Precision Electromagnetic Measurements (CPEM) pp 1–2
- [37] Kieler O F, Behr R, Wendisch R, Bauer S, Palafox L and Kohlmann J 2015 Towards a 1 V Josephson Arbitrary Waveform Synthesizer *IEEE Trans. Appl. Supercond.* 25 1–5
- [38] Benz S, Burroughs C and Dresselhaus P 2001 AC coupling technique for Josephson waveform synthesis *IEEE Trans*. *Appl. Supercond.* 11 612–6
- [39] Kučera J, Kováč J, Palafox L, Behr R and Vojáčková L 2020 Characterization of a precision modular sinewave generator Meas. Sci. Technol. 31 064002
- [40] Nissila J, Šíra M, Lee J, Öztürk T, Arifovic M, de Aguilar J D, Lapuh R and Behr R 2016 Stable arbitrary waveform generator as a transfer standard for ADC calibration 2016

- Conf. on Precision Electromagnetic Measurements (CPEM 2016) pp 1–2
- [41] Sosso A and Roberto C 2000 Calibration of multimeters as voltage ratio standards 2000 Conf. on Precision Electromagnetic Measurements (CPEM 2000) pp 375–6
- [42] Swerlein R L 1991 A 10 ppm accurate digital ac measurement algorithm *Proc. NCSL* pp 17–36
- [43] Hill J and Deacon T 1968 Theory design and measurement of inductive voltage dividers *Proc. Inst. Electr. Eng.* 115 727–35
- [44] Hsu J C, Chen S F, Kuo C J and Hsiao M 2016 Calibration of inductive voltage dividers at power frequencies using an AC-PJVS 2016 Conf. on Precision Electromagnetic Measurements (CPEM 2016) pp 1–2
- [45] Ramm G, Moser H and Braun A 1999 A new scheme for generating and measuring active, reactive and apparent power at power frequencies with uncertainties of 2.5 × 10<sup>-6</sup> IEEE Trans. Instrum. Meas. 48 422–6
- [46] Cassiago C, Cerri R, Paglia G L and Sosso A 2004 Application of DMM linearity to DC volt traceability 2004 Conf. on Precision Electromagnetic Measurements pp 176–7
- [47] Mašláň S, Šíra M and Skalická T 2018 Precision buffer with low input capacitance 2018 Conf. on Precision Electromagnetic Measurements (CPEM 2018) (IEEE) pp 1–2
- [48] Georgakopoulos D, Budovsky I and Benz S P 2019 AC voltage measurements to 120 V with a Josephson arbitrary waveform synthesizer and an inductive voltage divider IEEE Trans. Instrum. Meas. 68 1935–40
- [49] Herick J, Bauer S, Behr R, Beug M F, Kieler O F O and Palafox L 2018 Calibration of an inductive voltage divider using pulse-driven Josephson arrays 2018 Conf. on Precision Electromagnetic Measurements (CPEM 2018) (Paris, France, 8–13 July 2018) (https://doi.org/10.1109/ CPEM.2018.8500789)
- [50] Kieler O F, Behr R, Schleussner D, Palafox L and Kohlmann J 2013 Precision comparison of sine waveforms with pulse-driven Josephson arrays *IEEE Trans. Appl.* Supercond. 23 1301404
- [51] Starkloff M, Bauer M, Schubert M, Lee J, Behr R, Palafox L, Schaidhammer L, Böck A and Fleischmann P 2018 The AC quantum voltmeter used for AC current calibrations 2018 Conf. on Precision Electromagnetic Measurements (CPEM 2018) (IEEE) pp 1–2
- [52] Ilić D, Behr R and Lee J 2020 Stability of AC current measurements using AC–DC shunts and the AC quantum voltmeter 24th IMEKO TC4 Int. Symp. (Palermo, Itlay, 14–16 September 2020) pp 369–73
- [53] Lee J, Behr R, Palafox L, Katkov A, Schubert M, Starkloff M and Böck A C 2013 An ac quantum voltmeter based on a 10 V programmable Josephson array *Metrologia* 50 612
- [54] Šíra M 2017 QWTB–software toolbox for sampling measurements (available at: https://qwtb.github.io/qwtb/)
- [55] Šíra M, Mašláň S and Nováková Zachovalová V 2016 QWTB–software tool box for sampling measurements Conf. on Precision Electromagnetic Measurements Digest (IEEE) p 2
- [56] Mathworks 2012 Matlab (available at: www.mathworks.com)
- [57] GNU Octave 2012 (available at: www.gnu.org/software/
- [58] Mašláň S 2022 TWM tool (available at: https://github.com/ smaslan/TWM)
- [59] Mašláň S and Power O 2019 Project trace PQM—traceable measurements of power and power quality parameters Cal Lab: Int. J. Metrol. Jan-Mar 2019 27–35

- [60] Witt T and Reymann D 2000 Using power spectra and Allan variances to characterise the noise of Zener-diode voltage standards IEE Proc.-Sci. Meas. Technol. 147 177–82
- [61] Šíra M 2020 Noise and stability of Fluke 8588A in digitizing mode 2020 Conf. on Precision Electromagnetic Measurements (CPEM) pp 1–2
- [62] Snyder J J 1981 An ultra-high resolution frequency meter Proc. 35th Annual Frequency Control Symp. (Electronic Industries Association) pp 464–9
- [63] Fluke Corporation 2019 8588A / 8558A A reference multimeter and 8 1/2 digit multimeter operators manual (Everett, WA: Fluke Corporation)
- [64] Salinas J, de Aguilar J D, García-Lagos F, Joya G, Sanmamed Y A, Caballero R, Neira M and Sandoval F 2018 Study of Keysight 3458A temperature coefficient for different aperture times in DCV sampling mode 2018 Conf. on Precision Electromagnetic Measurements (CPEM 2018) (IEEE) pp 1–2
- [65] Sanmamed Y, Salinas J, de Aguilar J D, García-Lagos F and Caballero R 2019 Temperature influence on the frequency response of the Keysight 3458A digital multimeter *IMEKO* 2019 (Xi'an) (Xi'an, China, 17–20 September 2019)
- [66] National Instruments 2018 NI 2018 PXI/PCI-5922 specification (https://doi.org/10.1088/0957-0233/23/12/ 124002)
- [67] Behr R and Palafox L 2021 An AC quantum voltmeter for frequencies up to 100 kHz using sub-sampling *Metrologia* 58 025010
- [68] Peral D, Sanmamed Y A and Díaz de Aguilar J 2022 Feasibility of a digital counterpart of thermal converterbased current step up *IMEKO 2022 (Brescia, Italy)*
- [69] Peral D, Díaz de Aguilar J, Behr R, Ilic D, Kieler O, Herick J and Sanmamed Y A 2022 Quantum validation of digital step up of shunts CPEM 2022 (Wellington, New Zealand)
- [70] JCGM 1995 Evaluation of measurement data-guide to the expression of uncertainty in measurement (Bureau International des Poids et Measures) (available at: www. bipm.org/en/publications/guides/)
- [71] JCGM 2008 Evaluation of measurement data-supplement 1 to the "Guide to the expression of uncertainty in measurement"-propagation of distributions using a monte carlo method (Bureau International des Poids et Measures) (available at: www.bipm.org/en/publications/guides/)
- [72] JCGM 2011 Evaluation of measurement data—supplement 2 to the "Guide to the expression of uncertainty in measurement"—extension to any number of output quantities (Bureau International des Poids et Measures) (available at: www.bipm.org/en/publications/guides/)
- [73] Lapuh R, Šíra M, Lindič M and Voljč B 2016 Uncertainty of the signal parameter estimation from sampled data *Conf. on Precision Electromagnetic Measurements Digest* p 2
- [74] Slepicka D, Agrez D, Lapuh R, Nunzi E, Petri D, Radil T, Schoukens J and Sedlacek M 2010 Comparison of nonparametric frequency estimators *Instrumentation and Measurement Technology Conf. (I2MTC)*, 2010 IEEE (IEEE) pp 73–77
- [75] Šíra M, Mašláň S and Skalická T 2018 Uncertainty of phasor measurement unit calculated by means of monte carlo method 2018 Conf. on Precision Electromagnetic Measurements (CPEM 2018) (IEEE) pp 1–2
- [76] TracePQM Consortium 2018 TWM correction datasets reference manual (available at: https://github.com/smaslan/ TWM)
- [77] Horska J, Maslan S, Streit J and Sira M 2014 A Validation of a THD measurement e quipment with a 24-bit digitizer 2014 Conf. on Precision Electromagnetic Measurements (CPEM 2014) pp 502–3